Inorganic Chemistry

pubs.acs.org/IC
Article

Analyzing Fluoride Binding by Group 15 Lewis Acids: Pnictogen Bonding in the Pentavalent State

Logan T. Maltz and François P. Gabbaï*

Cite This: *Inorg. Chem.* 2023, 62, 13566−13572
Read Online

ABSTRACT: We report the results of a computational investigation into fluoride binding by a series of pentavalent pnictogen Lewis acids: pnictogen pentahalides (PnX_5), tetraphenyl pnictogeniums ($PnPh_4^+$), and triphenyl pnictogen tetrachlorocatecholates ($PnPh_3Cat$). Activation strain and energy decomposition analyses of the Lewis adducts not only clearly delineate the electrostatic and orbital contributions to these acid−base interactions but also highlight the importance of Pauli repulsion and molecular flexibility in determining relative Lewis acidity among the pnictogens.

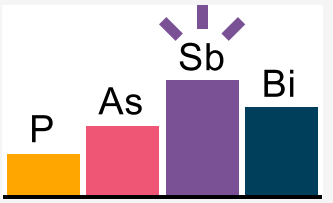

INTRODUCTION

Among Lewis acids, antimony holds a special place. SbF_5, in particular, is a Lewis superacid[1] that has had profound impacts on chemistry as exemplified by the work of Olah involving magic acid.[2] Recently, our group[3] and others[4] have effectively employed the unique Lewis acidity of Sb to develop transmembrane anion transporters and anion-recognition platforms. But what is it that distinguishes Sb from the other elements in the pnictogen (Pn) group? As chemists, we turn to chemical bonding and the competition between covalency and ionicity to answer this question.

Being saturated or hypervalent, pentavalent pnictogens use an empty σ^*-orbital to accept electron density. At the same time, the coincident σ-hole provides Coulombic stabilization to the newly formed linkage. Scheiner details the importance of these effects in his original definition of the pnictogen bond using trivalent elements[5] which has since expanded to include the interactions between any pnictogen-based Lewis acid—in the trivalent or pentavalent state—and a Lewis base.[6] Obviously, the distinction between the pnictogens must rely on amplification of whichever form of bonding predominates. Is the interaction more covalent? Then we might look to relative lowest-unoccupied molecular orbital (LUMO) energies to provide insight into the increasing Lewis acidity down the group.[7] Does ionicity dominate the bonding interaction? Then we might look to measures of the electrostatic potential to understand the increased Lewis acidity of Sb derivatives.

Wanting simple, intuitive descriptions of chemical bonding, we sometimes forget its complexity. Fortunately, chemists have developed models to better conceptualize complex interactions. Computational energy decomposition analysis (EDA) provides a convenient way to break an interaction into various energetic contributions: London dispersion interactions (ΔE_{disp}), electrostatic interactions (ΔE_{el}), orbital interactions (ΔE_{oi}), and Pauli repulsion (ΔE_{Pauli}). In our constant debates about the covalency or ionicity of an interaction, we often neglect London dispersion and Pauli repulsion.

Hypervalent SbF_5 reminds us that with any interaction—but especially closed-shell interactions—we need to consider Pauli repulsion: the destabilizing interaction occurring when two filled orbitals interact with each other. This repulsion is the underlying electronic basis for what we term "steric interactions" and is also at play in our discussions of ionic and covalent bonding. In this paper, we contend that Pauli repulsion rivals electrostatic and orbital interaction contributions in its importance to the Lewis acidity of the pnictogens.

In the past decade, the utility of the activation strain model (ASM) has been repeatedly demonstrated.[8] This model bifurcates the overall interaction energy ΔE into the energy necessary to strain and reorganize the interacting species into their interacting geometries (ΔE_{strain}) and the energy associated with allowing these strained species to interact (ΔE_{int}).[8a] To fully understand the interactions in these systems, ΔE_{int} is then parsed into its constituent components using EDA in the Amsterdam Density Functional (ADF) program (Figure 1). This method conveniently captures ΔE_{strain} and ΔE_{Pauli} which are important components of the overall interaction energy that are often overlooked because they are not as comfortably approachable as ΔE_{el} and ΔE_{oi}.

Inspired by Bickelhaupt and co-workers' analysis of trivalent pnictogen trihalides,[9] we have undertaken a similar analysis on a series of pentavalent pnictogen Lewis acids: pnictogen pentahalides (PnX_5), tetraphenyl pnictogeniums ($PnPh_4^+$), and triphenyl pnictogen tetrachlorocatecholates ($PnPh_3Cat$) (Figure 1). The last two families of compounds were selected because of their extensive use by our group as anion-binding

Received: June 16, 2023
Published: August 8, 2023

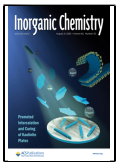

https://doi.org/10.1021/acs.inorgchem.3c01987
Inorg. Chem. 2023, 62, 13566−13572

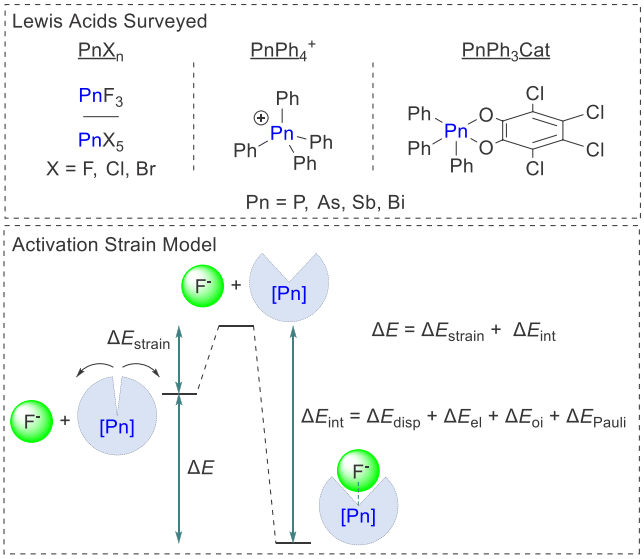

Figure 1. Top: Lewis acids surveyed in this study. Bottom: diagram of the activation strain model and the energy components comprising the overall interaction energy between the Lewis acids studied and F^-.

platforms, anion sensors, and anion transporters.[3] Unlike the previous work on trivalent pinctogens,[9] we expanded the scope of Lewis acids beyond the homoleptic halides but narrowed the scope of Lewis bases, focusing on these acids' interactions with fluoride (F^-). As such, we are effectively decomposing fluoride ion affinities (FIAs), though we are assessing changes in electronic energy (ΔE) while FIAs are defined as changes in enthalpy (ΔH).

The computations and analyses presented in this article illustrate that despite having lower magnitudes of stabilizing contributions from ΔE_{el} and ΔE_{oi}, Sb displays the highest Lewis acidity (most negative ΔE) in almost every case analyzed, the only exception being the trivalent pnictogen trifluorides. This result is due to Sb also having lower magnitudes of destabilizing contributions from ΔE_{strain} and ΔE_{Pauli}.

COMPUTATIONAL METHODS

For computational efficiency, we optimized the initial geometries of the Lewis acids and their fluoride adducts in Orca 5.0.2[10] using PBEh-3c/def2-mSVP[11] with the default defgrid2 settings. Frequency calculations were performed at the same level of theory to verify that all optimized structures were at a local minimum on the potential energy surface. Natural population analysis (NPA) charges were obtained through Natural Bonding Orbital calculations using NBO 7.0 at the same level of theory.[12] Where possible, structures were reoptimized from previously optimized coordinates.[9,13] All other structures were initially produced using either GaussView 6.1.1[14] or Avogadro[15] or by substituting one atom for another in the input file before performing the optimization depending on which method was simpler. For the F^- adducts of the $PnPh_3Cat$ species, two isomers were possible: F *trans* to Ph or F *trans* to O in the tetrachlorocatecholate. In the main text, the isomer with F *trans* to Ph is discussed as it is the lowest-energy isomer for Sb and similar trends are seen among both isomers. For completeness, both isomers were fully analyzed, and that data is presented in Table S1 and Graphs S7−S9.

The structures optimized in Orca were used as inputs for single-point energy calculations and EDA[16] computations conducted in ADF 2022.101[17] using the M06 functional[18] paired with the D3 model to account for dispersion effects.[19] The QZ4P basis set[20] as implemented in the ADF program was used without frozen-core approximation and with good numerical quality. The zeroth-order regular approximation (ZORA) Hamiltonian was employed to account for scalar relativistic effects.[21] To avoid numerical issues, the "Fix Dependencies" function in ADF was enabled for the $PnPh_4^+$ and $PnPh_3Cat$ species due to their size. ΔE_{strain} was determined by subtracting the single-point energy of the free Lewis acid from the single-point energy of the strained Lewis acid with no F^- bound. EDA directly provided ΔE_{disp}, ΔE_{el}, ΔE_{oi}, and ΔE_{Pauli}. LUMO energies were obtained from ADF as well.

Because EDA divides the Lewis adduct into its constituent acid and the small, highly negative F^- base, we used the counterpoise method

Table 1. Activation Strain and Energy Decomposition Analyses (in kcal mol^{-1}) at Optimized Geometries[a]

Acid	ΔE	ΔE_{strain}	ΔE_{int}	ΔE_{el}	ΔE_{oi}	ΔE_{Pauli}	$d_{Pn\cdots F}$ (Å)	Charge[b]	E_{LUMO} (eV)[c]
				$F^-\cdots PnF_3$					
PF_3	−49.6	18.5	−68.1	−173.2	−125.6	230.7	1.738[d]	1.77	−2.16
AsF_3	−60.1	10.2	−70.4	−161.9	−95.3	186.8	1.847[d]	1.84	−2.50
SbF_3	−71.2	9.0	−80.2	−161.0	−81.5	162.2	1.989[d]	1.98	−3.03
BiF_3	−72.9	5.8	−78.7	−142.9	−62.9	127.1	2.119[d]	2.00	−2.94
				$F^-\cdots PnF_5$					
PF_5	−91.6	51.8	−143.4	−220.1	−154.1	230.9	1.634	2.71	−5.49
AsF_5	−104.5	33.0	−137.5	−215.1	−129.8	207.5	1.738	2.76	−6.37
SbF_5	−120.3	23.7	−144.1	−209.3	−101.4	166.7	1.900	2.96	−6.52
BiF_5	−116.9	17.3	−134.1	−194.2	−92.4	152.6	1.997	2.80	−7.34
				$F^-\cdots PnPh_4^+$					
PPh_4^+	−125.4	33.3	−158.7	−251.1	−155.8	248.7	1.724	1.52	−5.37
$AsPh_4^+$	−123.4	23.7	−147.1	−230.8	−118.9	203.2	1.852	1.64	−5.32
$SbPh_4^+$	−142.0	18.6	−160.6	−229.4	−102.2	171.4	2.000	1.94	−5.81
$BiPh_4^+$	−138.9	14.2	−153.0	−206.1	−84.9	138.3	2.132	1.78	−6.01
				$F^-\cdots PnPh_3Cat$[e]					
PPh_3Cat	−75.0	31.3	−106.3	−199.4	−170.2	263.8	1.683	1.76	−2.94
$AsPh_3Cat$	−73.2	20.6	−93.8	−180.5	−135.3	222.5	1.801	1.89	−3.13
$SbPh_3Cat$	−85.9	16.0	−101.8	−172.4	−112.9	184.0	1.955	2.23	−3.30
$BiPh_3Cat$	−78.8	12.8	−91.6	−152.1	−98.7	159.6	2.065	2.05	−3.69

[a] ΔE_{disp} omitted for clarity. [b] NPA charge in strained acid without F^-. [c] LUMO energy in strained acid without F^-. [d] Smaller of two Pn···F distances. [e] Isomer with F *trans* to Ph. For the complete table, see Table S1 in the Supporting Information.

https://doi.org/10.1021/acs.inorgchem.3c01987
Inorg. Chem. 2023, 62, 13566−13572

Chart 1. Bar Graph Depicting the Data from the Activation Strain and Energy Decomposition Analyses of the $F^-\cdots PnF_3$ and $F^-\cdots PnF_5$ Series[a]

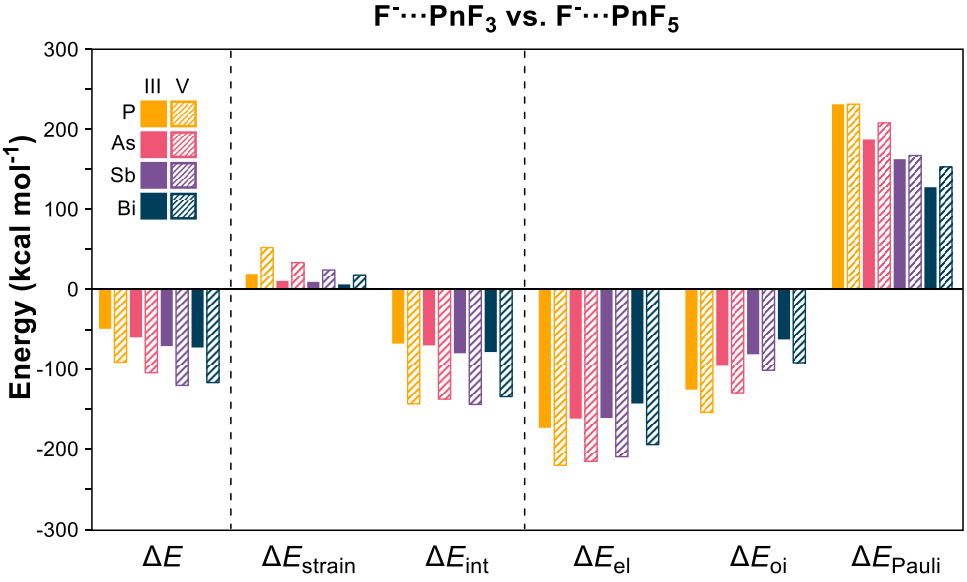

[a] ΔE_{disp} has been omitted for clarity.

as implemented in ADF to investigate the basis set superposition error (BSSE).[22] The BSSE was determined to be in the narrow range of 2.88−3.74 kcal mol^{-1} for all species, predominantly due to F^-, with the Lewis acid contributing ≤0.3 kcal mol^{-1} to the BSSE in all cases. In accordance with prior EDA investigations of main group Lewis acid adducts,[9,23] the individual BSSEs were not incorporated in the reported energy values. As expected for a hard ion such as F^-, ΔE_{disp} is negligible for all Lewis acids considered, reaching a maximum magnitude of −0.5 kcal mol^{-1} in the $PnPh_4^+$ and $PnPh_3Cat$ species which is expected given their larger surface areas (Table S1).

RESULTS AND DISCUSSION

Our lab has previously demonstrated that oxidizing the pnictogen center from the +3 state to the +5 state increases its Lewis acidity.[3f] This conclusion is corroborated by the ∼40 kcal mol^{-1} increase in the magnitude of ΔE for all pnictogens going from PnF_3 to PnF_5 (Table 1). Gratifyingly, this data vindicates our assertion that oxidation leads to both an increase in the electrostatic contribution to the interaction through a deepening of the σ-hole and an increase in the orbital contribution through the lowering of the σ^*-based LUMO (Chart 1). Moving from PnF_3 to PnF_5, we also see an increase in ΔE_{strain} and ΔE_{Pauli} as expected with an increased number of substituents attached to the central pnictogen and a decrease in the bond lengths upon oxidation. Thus, for oxidation from Pn^{III} to Pn^{V}, the substantial increase in stabilization energy leads to greatly enhanced Lewis acidity despite a simultaneous increase in destabilizing interactions. As we will discuss, this scenario is inverted when looking at the periodic trends across the pentavalent pnictogens.

We focus our analysis on the PnF_5 series as the trends seen hold for the other series. With a ΔE of −120.3 kcal mol^{-1}—in line with previously computed fluoride ion affinities[24]—SbF_5 is the strongest Lewis acid in this series. Down the group, there is a 28.7 kcal mol^{-1} increase in the magnitude of ΔE from −91.6 kcal mol^{-1} for PF_5. This general trend of increasing Lewis acidity down the group has been observed experimentally as well.[7,25] While the destabilization from ΔE_{strain} decreases from 51.8 kcal mol^{-1} for PF_5 to 23.7 kcal mol^{-1} for SbF_5, ΔE_{int} stays nearly constant, seeing only a 0.7 kcal mol^{-1} increase in magnitude.

The decrease in ΔE_{strain} follows from the larger size of the pnictogen center allowing increased flexibility of the coordinated ligands. This flexibility was highlighted in Moc and Morokuma's 1997 study on hypervalent pnictogens wherein they concluded that the larger pnictogens enjoy a reduced barrier to Berry pseudorotation due to an increased ease in adjusting their Pn−F bond lengths from the ground state D_{3h} structure to achieve the transitional C_{4v} structure.[26] Their values for the pseudorotation barrier are comparable to those calculated by Breidung and Thiel in 1992.[27] During this conversion from D_{3h} to C_{4v}, the predominantly ligand-based highest occupied molecular orbital (HOMO) decreases in energy while the pnictogen-centered HOMO−1 increases in energy.[28] Accordingly, decreasing the destabilization of the pnictogen-based HOMO−1 corresponds with a decrease in the pseudorotation barrier. Given this analysis, it seems that the most influential factor in the PnF_5 series is the weaker bonds formed down the group resulting from greater atomic radius and increased orbital diffuseness which both lead to less effective orbital overlap. Steric repulsion also plays a role in decreased ΔE_{strain} as larger atoms allow more room between the ligands as they become compressed in the C_{4v} geometry.

Turning our attention from ΔE_{strain}, we see that though the change in ΔE_{int} is small down the group, the magnitude of ΔE_{int} is 3-6 times greater than that of ΔE_{strain} and thus contributes significantly to ΔE. As expected with increased atomic radius, ΔE_{el} decreases consistently down the group with SbF_5 having an electrostatic contribution that is 10.8 kcal mol^{-1} less stabilizing than that for PF_5. ΔE_{oi} sees a dramatic decrease of 52.7 kcal mol^{-1} in stabilization going from PF_5 to SbF_5, which can be attributed to the increased diffuseness of the pnictogen center's orbitals leading to decreased overlap with the incoming Lewis base due to the size mismatch. This combination of increasing atomic radius and increasing orbital diffuseness progressively favors the ionic contribution down

https://doi.org/10.1021/acs.inorgchem.3c01987
Inorg. Chem. 2023, 62, 13566−13572

the group with ΔE_{el} increasing from 59% of the stabilizing contribution for PF_5 to 67% for SbF_5.

Despite a cumulative 63.5 kcal mol^{-1} decrease in stabilization from P to Sb, there is a simultaneous 64.2 kcal mol^{-1} decrease in ΔE_{Pauli} that more than compensates, producing a ΔE_{int} that remains largely unchanged down the group which then allows the decrease in ΔE_{strain} to drive the observed differences in Lewis acidity . Similar trends are seen for the pentachloride and pentabromide species as well (Supporting Information). Noticeably lacking in this discussion, however, is Bi.

While BiF_5 is more Lewis acidic than PF_5 and AsF_5, there is a drop in Lewis acidity going from SbF_5 to BiF_5 which has also been observed experimentally and has been repeatedly reproduced in FIA calculations (Table 2).[7,25,26,29] The trends that exist down the group still hold when going from Sb to Bi: both stabilizing and destabilizing contributions decrease. This transition, however, does not come with the same magnitude of change in the energetic contributions—the decrease in destabilizing contributions no longer compensates as much for the decrease in stabilizing contributions. While ΔE_{el} decreases from P to As by 2% and then from As to Sb by 3%, there is a significant 7% decrease in ΔE_{el} from Sb to Bi. This decrease appears less consequential upon realizing that ΔE_{oi} only decreases by 9% from Sb to Bi compared to a 22% decrease from As to Sb. As a result, Sb and Bi have similar ratios of ΔE_{el} to ΔE_{oi} with both having ∼32% of the stabilization energy coming from ΔE_{oi}.

Table 2. Comparison of ΔE and FIAs (in kcal mol^{-1})

Acid	ΔE	FIA
PF_3	−49.6	47.8[a]
AsF_3	−60.1	58.3[a]
SbF_3	−71.2	69.3[a]
BiF_3	−72.9	
PF_5	−91.6	91.9[b]
AsF_5	−104.5	104.1[b]
SbF_5	−120.3	117.6[b]
BiF_5	−116.9	115.2[b]

[a]FIAs converted from kJ mol^{-1} from ref 24b. [b]FIAs obtained as negatives of the reaction energy for $PnF_5 + F^- \rightarrow PnF_6^-$ in ref 26.

The major difference between Sb and Bi lies in the reduction of ΔE_{Pauli}. ΔE_{strain} decreases rather consistently: a 28% decrease from As to Sb and a 27% decrease from Sb to Bi. This steady decrease is likely due to the predictably weaker and longer bonds formed by the more diffuse orbitals moving down the group. ΔE_{Pauli}, on the other hand, only decreases by 8% from Sb to Bi compared to the significant 20% decrease seen from As to Sb. This inconsistency results from the unexpected trend in covalent radii. The covalent radius from As to Sb increases by 0.20 Å (1.19 vs 1.39 Å).[30] Due to the lanthanide contraction, the increase from Sb to Bi is only 0.09 Å (1.39 vs 1.48 Å)—also reflected in the computed Pn−F bond lengths (Table 1).[30]

With a smaller-than-expected increase in size, the Bi−F bonds are closer to the incoming F^- than might otherwise be anticipated leading to the smaller-than-expected decrease in Pauli repulsion. As such, the larger-than-expected Pauli repulsion is not as effectively counterbalanced by the stabilizing contributions in Bi as it is in Sb, leading to a reduction in overall Lewis acidity. Owing to the scandide contraction, a similarly small decrease of 10% in ΔE_{Pauli} is seen for the transition from P to As; however, this 10% decrease corresponds to a considerable 23.4 kcal mol^{-1} reduction in ΔE_{Pauli} while the 8% drop from Sb to Bi only produces a 14.1 kcal mol^{-1} decrease, indicating that an increase in covalent radius has a more profound effect on ΔE_{Pauli} for smaller atoms.

With these trends in mind, we turn to more complex pnictogen-based Lewis acids, starting with the $PnPh_4^+$ series. These cationic species serve as representative examples of pnictogen-based Lewis acids employed extensively in anion transport.[3g] For these cationic species—and the rest of the species studied—ΔE seems to oscillate: Sb and Bi have larger ΔE's than P and As with Bi and As having the lower ΔE's in these pairs (Chart 2). While this "secondary periodicity" is also seen in the ΔE_{int} of the PnF_5 series, it likely manifests in the ΔE of the $PnPh_4^+$ series due to a slight increase in the importance of ΔE_{el} as a result of the cationic charge.[31] The percentage of ΔE_{el}'s contribution to the stabilization energy increases from 59−68% in the PnF_5 series to 62−71% in the $PnPh_4^+$ series. Furthermore, ΔE_{el} increases in magnitude by ∼20−30 kcal mol^{-1} for P and Sb but only ∼12−16 kcal mol^{-1} for As and Bi. This observed secondary periodicity results from the scandide contraction at As and the lanthanide contraction at Bi which lead to not only smaller radii than would be expected but also higher electronegativities than expected.

While electronegativity seemingly decreases down the group according to the Pauling scale, Haïssinsky reminds us that electronegativity increases with oxidation state, leading to electronegativities of 2.2 for As^V, 2.1 for Sb^V, and >2.3 for Bi^V.[32] This irregularity in the electronegativity is seen in the natural population analysis (NPA) charges in the strained geometries: +1.52 for P, +1.64 for As, +1.94 for Sb, and +1.78 for Bi (Table 1). Though there is a slight increase in charge from P to As, it cannot overcome the 0.12 Å increase in covalent radius,[30] resulting in a large 20.3 kcal mol^{-1} decrease in ΔE_{el} for this pair. The transition from Sb to Bi sees an even larger decrease of 23.3 kcal mol^{-1} in ΔE_{el} due to the combination of decreased positive charge at the pnictogen center and increased covalent radius (0.09 Å).[30] Ultimately, these large changes in ΔE_{el} are reflected in ΔE due to the increased prominence of electrostatic contributions in these cationic species.

Despite the apparent increased importance of ΔE_{el} in determining ΔE, $SbPh_4^+$—even with its lower ΔE_{el}—is still 16.6 kcal mol^{-1} more acidic than PPh_4^+. While the stabilizing interactions (ΔE_{el} + ΔE_{oi}) decrease by 75.3 kcal mol^{-1}, they are matched by a 77.3 kcal mol^{-1} decrease in ΔE_{Pauli}. The 14.7 kcal mol^{-1} decrease in ΔE_{strain} then drives the increased Lewis acidity of $SbPh_4^+$.

Finally, we analyzed the neutral $PnPh_3Cat$ series. Oxidation of pnictogens using *ortho*-chloranil has been repeatedly applied to produce active anion receptors and Lewis acid catalysts.[3f,13] Due to the differing substituents, two isomers are possible upon binding F^-: one where F is *trans* to Ph and the other with F *trans* to Cat. Because the same trends hold in both series (Supporting Information) and the isomer with F *trans* to Ph is 1.5 kcal mol^{-1} lower in energy for Sb, we have focused our analysis on this series. Overall, these ΔE values are lower than their PnF_5 and $PnPh_4^+$ counterparts yet still higher than those seen for the pnictogen trifluorides. This decreased Lewis acidity is expected due to a reduced σ-hole and a higher-lying σ^*-orbital resulting from decreased bond polarity. This reduced polarity produces a less ionic interaction as seen in

https://doi.org/10.1021/acs.inorgchem.3c01987
Inorg. Chem. 2023, 62, 13566−13572

Chart 2. Bar Graphs Depicting the Data from the Activation Strain and Energy Decomposition Analyses of the $F^-\cdots PnPh_4^+$ (Top) and $F^-\cdots PnPh_3Cat$ (Bottom) Series[a]

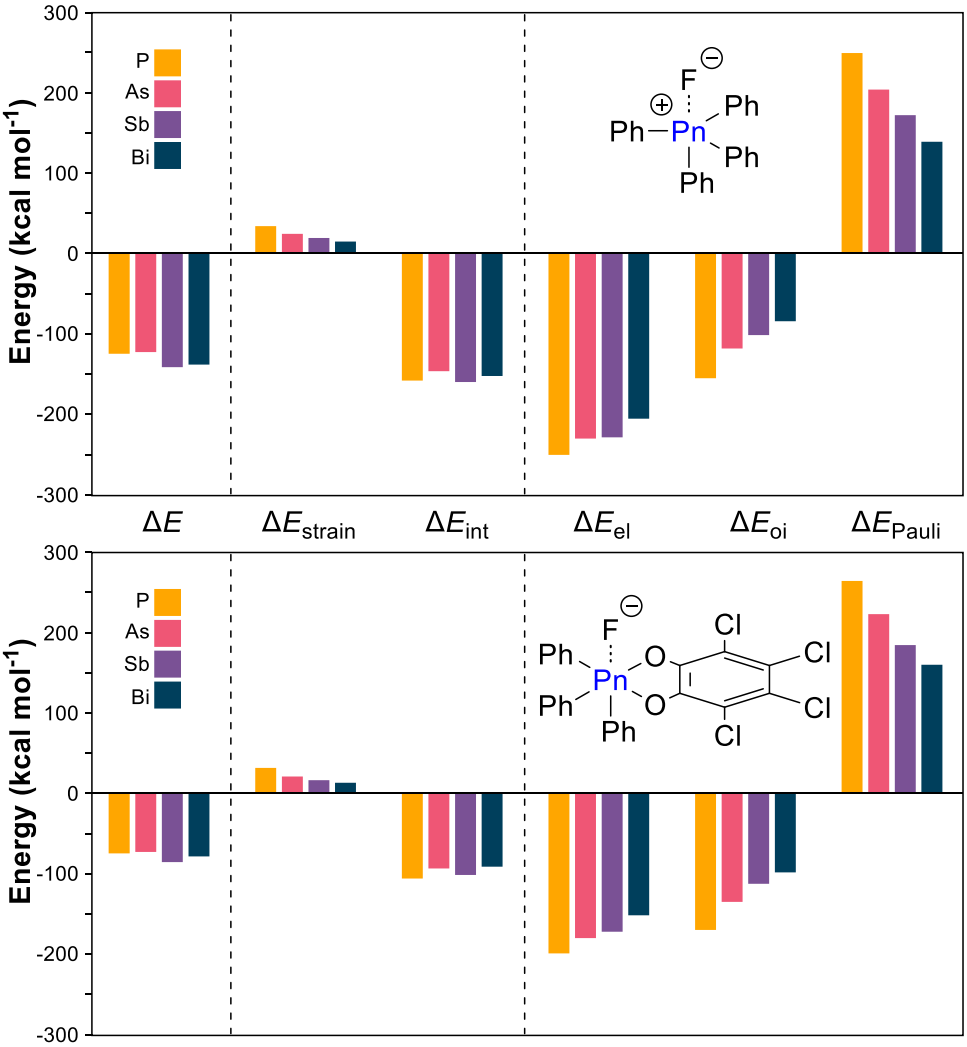

[a] ΔE_{disp} has been omitted for clarity.

the relative contributions of ΔE_{el} and ΔE_{oi}: ΔE_{oi} contributes 39−46% to the stabilization energy for all pnictogens, whereas it contributes 29−41% in the PnF_5 and $PnPh_4^+$ series (Chart 2). While the overall ΔE values are lower in the $PnPh_3Cat$ series, it is noteworthy that ΔE_{strain} is the lowest among the pentavalent pnictogen series presented in Table 1, indicating the benefits of preorganization that the catecholate provides.[23] As also seen in the PnF_5 and $PnPh_4^+$ series, Sb has the greatest Lewis acidity despite having the lowest magnitude of stabilizing contributions due to such a significant reduction in destabilizing contributions.

CONCLUSIONS

Though FIAs provide a way to compare the strengths of Lewis acids, activation strain analysis paired with EDA allows deeper insight into the underlying contributions to Lewis acid strength. We have confirmed that oxidation from Pn^{III} to Pn^{V} produces an increase in ΔE_{el} and ΔE_{oi} due to a deeper σ-hole and a lower-energy σ^*-orbital. While it was already known that Sb-based acids are strong Lewis acids, our analysis highlights the significance of increased molecular flexibility and decreased Pauli repulsion in the preeminence of Sb among the pentavalent pnictogens. Despite lower stabilizing contributions from ΔE_{el} and ΔE_{oi} moving down the group, Sb exhibits greater Lewis acidity due to lower destabilizing contributions from ΔE_{strain} and ΔE_{Pauli}. The decrease in ΔE_{Pauli} prevents drastic changes in ΔE_{int} by offsetting the decreases in ΔE_{el} and ΔE_{oi}, thereby allowing the significant reduction in ΔE_{strain} to drive the dramatic increase in ΔE from P to Sb. Additionally, we not only confirmed the importance of electrostatic contributions for cationic Lewis acids but also demonstrated that the pnictogen bond has substantial orbital contribution. Our hope is that this work informs future applications of pnictogen-based Lewis acids.

ASSOCIATED CONTENT

Supporting Information

The Supporting Information is available free of charge at https://pubs.acs.org/doi/10.1021/acs.inorgchem.3c01987.

Complete data table; bar graphs; and optimized structures in *XYZ* format (PDF)

https://doi.org/10.1021/acs.inorgchem.3c01987
Inorg. Chem. 2023, 62, 13566−13572

AUTHOR INFORMATION

Corresponding Author

François P. Gabbaï − *Department of Chemistry, Texas A&M University, College Station, Texas 77843, United States;* orcid.org/0000-0003-4788-2998; Email: francois@tamu.edu

Author

Logan T. Maltz − *Department of Chemistry, Texas A&M University, College Station, Texas 77843, United States*

Complete contact information is available at: https://pubs.acs.org/10.1021/acs.inorgchem.3c01987

Author Contributions

L.T.M. conducted the computational work and data analysis. F.P.G. oversaw the study. L.T.M. and F.P.G. wrote the manuscript.

Notes

The authors declare no competing financial interest.
A draft of this work has been deposited to ChemRxiv.[33]

ACKNOWLEDGMENTS

This work was performed with support from the National Science Foundation (CHE-2108728), the Welch Foundation (A-1423), and Texas A&M University (Arthur E. Martell Chair of Chemistry). This research was conducted with the advanced computing resources provided by Texas A&M High-Performance Research Computing.

REFERENCES

(1) Greb, L. Lewis Superacids: Classifications, Candidates, and Applications. *Chem. - Eur. J.* **2018**, *24*, 17881−17896.

(2) (a) Olah, G. A.; Schlosberg, R. H. Chemistry in super acids. I. Hydrogen exchange and polycondensation of methane and alkanes in FSO_3H-SbF_5 ("magic acid") solution. Protonation of alkanes and the intermediacy of CH_5^+ and related hydrocarbon ions. The high chemical reactivity of "paraffins" in ionic solution reactions. *J. Am. Chem. Soc.* **1968**, *90*, 2726−2727. (b) Olah, G. A. *Superacid Chemistry*; Wiley: Hoboken, N.J, 2009.

(3) (a) Ke, I.-S.; Myahkostupov, M.; Castellano, F. N.; Gabbaï, F. P. Stibonium Ions for the Fluorescence Turn-On Sensing of F^- in Drinking Water at Parts per Million Concentrations. *J. Am. Chem. Soc.* **2012**, *134*, 15309−15311. (b) Hirai, M.; Gabbaï, F. P. Lewis acidic stiborafluorenes for the fluorescence turn-on sensing of fluoride in drinking water at ppm concentrations. *Chem. Sci.* **2014**, *5*, 1886−1893. (c) Hirai, M.; Gabbaï, F. P. Squeezing Fluoride out of Water with a Neutral Bidentate Antimony(V) Lewis Acid. *Angew. Chem., Int. Ed.* **2015**, *54*, 1205−1209. (d) Hirai, M.; Myahkostupov, M.; Castellano, F. N.; Gabbaï, F. P. 1-Pyrenyl- and 3-Perylenyl-antimony(V) Derivatives for the Fluorescence Turn-On Sensing of Fluoride Ions in Water at Sub-ppm Concentrations. *Organometallics* **2016**, *35*, 1854−1860. (e) Chen, C.-H.; Gabbaï, F. P. Fluoride Anion Complexation by a Triptycene-Based Distiborane: Taking Advantage of a Weak but Observable C−H···F Interaction. *Angew. Chem., Int. Ed.* **2017**, *56*, 1799−1804. (f) Yang, M.; Tofan, D.; Chen, C.-H.; Jack, K. M.; Gabbaï, F. P. Digging the Sigma-Hole of Organoantimony Lewis Acids by Oxidation. *Angew. Chem., Int. Ed.* **2018**, *57*, 13868−13872. (g) Park, G.; Brock, D. J.; Pellois, J.-P.; Gabbaï, F. P. Heavy Pnictogenium Cations as Transmembrane Anion Transporters in Vesicles and Erythrocytes. *Chem* **2019**, *5*, 2215−2227. (h) Gonzalez, V. M.; Park, G.; Yang, M.; Gabbaï, F. P. Fluoride anion complexation and transport using a stibonium cation stabilized by an intramolecular P═O → Sb pnictogen bond. *Dalton Trans.* **2021**, *50*, 17897−17900.

(4) (a) Robertson, A. P. M.; Chitnis, S. S.; Jenkins, H. A.; McDonald, R.; Ferguson, M. J.; Burford, N. Establishing the Coordination Chemistry of Antimony(V) Cations: Systematic Assessment of $Ph_4Sb(OTf)$ and $Ph_3Sb(OTf)_2$ as Lewis Acceptors. *Chem. - Eur. J.* **2015**, *21*, 7902−7913. (b) Chitnis, S. S.; Sparkes, H. A.; Annibale, V. T.; Pridmore, N. E.; Oliver, A. M.; Manners, I. Addition of a Cyclophosphine to Nitriles: An Inorganic Click Reaction Featuring Protio, Organo, and Main-Group Catalysis. *Angew. Chem., Int. Ed.* **2017**, *56*, 9536−9540. (c) Qiu, J.; Song, B.; Li, X.; Cozzolino, A. F. Solution and gas phase evidence of anion binding through the secondary bonding interactions of a bidentate bis-antimony(III) anion receptor. *Phys. Chem. Chem. Phys.* **2018**, *20*, 46−50. (d) Benz, S.; Poblador-Bahamonde, A. I.; Low-Ders, N.; Matile, S. Catalysis with pnictogen, chalcogen, and halogen bonds. *Angew. Chem., Int. Ed.* **2018**, *57*, 5408−5412. (e) Sharma, D.; Balasubramaniam, S.; Kumar, S.; Jemmis, E. D.; Venugopal, A. Reversing Lewis acidity from bismuth to antimony. *Chem. Commun.* **2021**, *57*, 8889−8892. (f) Sharma, D.; Benny, A.; Gupta, R.; Jemmis, E. D.; Venugopal, A. Crystallographic evidence for a continuum and reversal of roles in primary−secondary interactions in antimony Lewis acids: applications in carbonyl activation. *Chem. Commun.* **2022**, *58*, 11009−11012.

(5) Scheiner, S. A new noncovalent force: Comparison of P···N interaction with hydrogen and halogen bonds. *J. Chem. Phys.* **2011**, *134*, No. 094315.

(6) Varadwaj, A.; Varadwaj, P. R.; Marques, H. M.; Yamashita, K. Definition of the Pnictogen Bond: A Perspective. *Inorganics* **2022**, *10*, No. 149.

(7) Gillespie, R. J.; Ouchi, K.; Pez, G. P. Fluorosulfuric acid solvent system. VI. Solutions of phosphorus, arsenic, bismuth, and niobium pentafluorides and titanium tetrafluoride. *Inorg. Chem.* **1969**, *8*, 63−65.

(8) (a) van Zeist, W.-J.; Bickelhaupt, F. M. The activation strain model of chemical reactivity. *Org. Biomol. Chem.* **2010**, *8*, 3118−3127. (b) Vermeeren, P.; van der Lubbe, S. C. C.; Guerra, C. F.; Bickelhaupt, F. M.; Hamlin, T. A. Understanding chemical reactivity using the activation strain model. *Nat. Protoc.* **2020**, *15*, 649−667.

(9) de Azevedo Santos, L.; Hamlin, T. A.; Ramalho, T. C.; Bickelhaupt, F. M. The pnictogen bond: a quantitative molecular orbital picture. *Phys. Chem. Chem. Phys.* **2021**, *23*, 13842−13852.

(10) (a) Neese, F. The ORCA program system. *WIREs Comput. Mol. Sci.* **2012**, *2*, 73−78. (b) Neese, F.; Wennmohs, F.; Becker, U.; Riplinger, C. The ORCA quantum chemistry program package. *J. Chem. Phys.* **2020**, *152*, No. 224108. (c) Neese, F. Software update: The ORCA program system—Version 5.0. *WIREs Comput. Mol. Sci.* **2022**, *12*, No. e1606.

(11) Grimme, S.; Brandenburg, J. G.; Bannwarth, C.; Hansen, A. Consistent structures and interactions by density functional theory with small atomic orbital basis sets. *J. Chem. Phys.* **2015**, *143*, No. 054107.

(12) Glendening, E. D.; Badenhoop, J. K.; Reed, A. E.; Carpenter, J. E.; Bohmann, J. A.; Morales, C. M.; Karafiloglou, P.; Landis, C. R.; Weinhold, F. *NBO 7.0, Theoretical Chemistry Institute*; University of Wisconsin: Madison, WI, 2018.

(13) (a) You, D.; Zhou, B.; Hirai, M.; Gabbaï, F. P. Distiboranes based on *ortho*-phenylene backbones as bidentate Lewis acids for fluoride anion chelation. *Org. Biomol. Chem.* **2021**, *19*, 4949−4957. (b) Chishiro, A.; Akioka, I.; Sumida, A.; Oka, K.; Tohnai, N.; Yumura, T.; Imoto, H.; Naka, K. Tetrachlorocatecholates of triarylarsines as a novel class of Lewis acids. *Dalton Trans.* **2022**, *51*, 13716−13724.

(14) Dennington, R.; Keith, T. A.; Millam, J. M. *GaussView*, version 6; Semichem Inc.: Shawnee Mission, KS, 2016.

(15) Hanwell, M. D.; Curtis, D. E.; Lonie, D. C.; Vandermeersch, T.; Zurek, E.; Hutchison, G. R. Avogadro: an advanced semantic chemical editor, visualization, and analysis platform. *J. Cheminf.* **2012**, *4*, No. 17.

(16) (a) Bickelhaupt, F. M.; Nibbering, N. M. M.; Van Wezenbeek, E. M.; Baerends, E. J. Central bond in the three $CN^{\bullet}$ dimers NC-CN, CN-CN and CN-NC: electron pair bonding and Pauli repulsion effects. *J. Phys. Chem. A* **1992**, *96*, 4864−4873. (b) Bickelhaupt, F. M.; Baerends, E. J.Kohn-Sham Density Functional Theory: Predicting and

Understanding Chemistry. In *Reviews in Computational Chemistry*; John Wiley & Sons, 2000; pp 1−86. (c) Krapp, A.; Bickelhaupt, F. M.; Frenking, G. Orbital Overlap and Chemical Bonding. *Chem. - Eur. J.* **2006**, *12*, 9196−9216.
(17) te Velde, G.; Bickelhaupt, F. M.; Baerends, E. J.; Fonseca Guerra, C.; van Gisbergen, S. J. A.; Snijders, J. G.; Ziegler, T. Chemistry with ADF. *J. Comput. Chem.* **2001**, *22*, 931−967.
(18) (a) Zhao, Y.; Truhlar, D. G. A new local density functional for main-group thermochemistry, transition metal bonding, thermochemical kinetics, and noncovalent interactions. *J. Chem. Phys.* **2006**, *125*, No. 194101. (b) Zhao, Y.; Truhlar, D. The M06 suite of density functionals for main group thermochemistry, thermochemical kinetics, noncovalent interactions, excited states, and transition elements: two new functionals and systematic testing of four M06-class functionals and 12 other functionals. *Theor. Chem. Acc.* **2008**, *120*, 215−241.
(19) (a) Grimme, S.; Antony, J.; Ehrlich, S.; Krieg, H. A consistent and accurate ab initio parametrization of density functional dispersion correction (DFT-D) for the 94 elements H-Pu. *J. Chem. Phys.* **2010**, *132*, No. 154104. (b) Grimme, S.; Hansen, A.; Brandenburg, J. G.; Bannwarth, C. Dispersion-Corrected Mean-Field Electronic Structure Methods. *Chem. Rev.* **2016**, *116*, 5105−5154.
(20) van Lenthe, E.; Baerends, E. J. Optimized Slater-type basis sets for the elements 1-118. *J. Comput. Chem.* **2003**, *24*, 1142−1156.
(21) van Lenthe, E.; Baerends, E. J.; Snijders, J. G. Relativistic total energy using regular approximations. *J. Chem. Phys.* **1994**, *101*, 9783−9792.
(22) Cramer, C. J. *Essentials of Computational Chemistry Theories and Models*, 2nd ed.; John Wiley & Sons Ltd.: Hoboken, NJ, 2004.
(23) Roth, D.; Stirn, J.; Stephan, D. W.; Greb, L. Lewis Superacidic Catecholato Phosphonium Ions: Phosphorus−Ligand Cooperative C−H Bond Activation. *J. Am. Chem. Soc.* **2021**, *143*, 15845−15851.
(24) (a) Krossing, I.; Raabe, I. Relative stabilities of weakly coordinating anions: A computational study. *Chem. - Eur. J.* **2004**, *10*, 5017−5030. (b) Erdmann, P.; Leitner, J.; Schwarz, J.; Greb, L. An Extensive Set of Accurate Fluoride Ion Affinities for p-Block Element Lewis Acids and Basic Design Principles for Strong Fluoride Ion Acceptors. *ChemPhysChem* **2020**, *21*, 987−994.
(25) Bougon, R.; Bui Huy, T.; Cadet, A.; Charpin, P.; Rousson, R. Adducts of chlorine oxide trifluoride with group V element pentafluorides. Structural study of the hexafluoro anions. *Inorg. Chem.* **1974**, *13*, 690−695.
(26) Moc, J.; Morokuma, K. Ab initio MO study on the periodic trends in structures and energies of hypervalent compounds: five-, six-, and seven-coordinated XF_5, XH_6^-, XF_6^-, XH_7^{2-} and XF_7^{2-} species containing a group 15 central atom (where X is P, As, Sb, Bi). *J. Mol. Struct.* **1997**, *436*−*437*, 401−418.
(27) Breidung, J.; Thiel, W. A systematic ab initio study of the group V trihalides MX_3 and pentahalides MX_5 (M = P—Bi, X = F—I). *J. Comput. Chem.* **1992**, *13*, 165−176.
(28) Gimarc, B. M. The shapes and other properties of non-transition element complexes. 3. AB_5. *J. Am. Chem. Soc.* **1978**, *100*, 2346−2353.
(29) Jupp, A. R.; Johnstone, T. C.; Stephan, D. W. Improving the Global Electrophilicity Index (GEI) as a Measure of Lewis Acidity. *Inorg. Chem.* **2018**, *57*, 14764−14771.
(30) Cordero, B.; Gomez, V.; Platero-Prats, A. E.; Reves, M.; Echeverria, J.; Cremades, E.; Barragan, F.; Alvarez, S. Covalent radii revisited. *Dalton Trans.* **2008**, 2832−2838.
(31) (a) Biron, E. V. Phenomena of secondary periodicity. *Zh. Russ. Fiz.-Khim. Obshch. Ch. Khim.* **1915**, *47*, 964−988. (b) Pyykkö, P. On the Interpretation of 'Secondary Periodicity" in the Periodic System. *J. Chem. Res.* **1979**, 380−381. (c) Lipshultz, J. M.; Li, G.; Radosevich, A. T. Main Group Redox Catalysis of Organopnictogens: Vertical Periodic Trends and Emerging Opportunities in Group 15. *J. Am. Chem. Soc.* **2021**, *143*, 1699−1721.
(32) (a) Haïssinsky, M. Échelle des électronégativités de Pauling et chaleurs de formation des composés inorganiques. *J. Phys. Radium* **1946**, *7*, 7−11. (b) Allred, A. L.; Hensley, A. L. Electronegativities of nitrogen, phosphorus, arsenic, antimony and bismuth. *J. Inorg. Nucl. Chem.* **1961**, *17*, 43−54.
(33) Maltz, L.; Gabbaï, F. P. Analyzing Fluoride Binding by Group 15 Lewis Acids: Pnictogen Bonding in the Pentavalent State *Chemrxiv* 2023, DOI: 10.26434/chemrxiv-2023-t60dq.

https://doi.org/10.1021/acs.inorgchem.3c01987
Inorg. Chem. 2023, 62, 13566−13572